Volume 49
Number 26
14 July 2020
Pages 8803-9168

Dalton Transactions

An international journal of inorganic chemistry

rsc.li/dalton

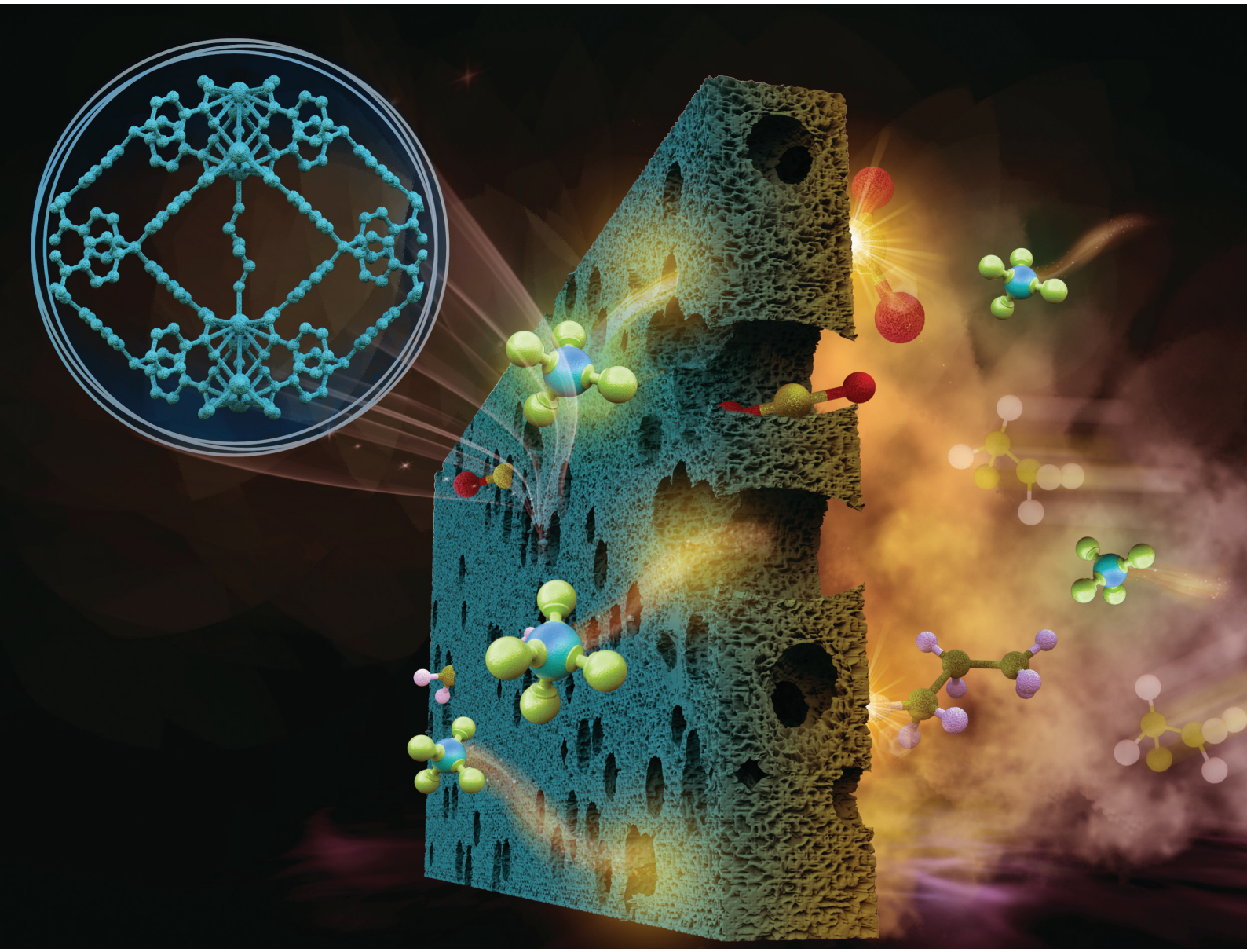

ISSN 1477-9226

ROYAL SOCIETY OF CHEMISTRY

COMMUNICATION

Mingyan Wu, Jing Li *et al.*

Building a robust 3D Ca-MOF by a new square Ca_4O SBU for purification of natural gas

Dalton Transactions

ROYAL SOCIETY OF CHEMISTRY

COMMUNICATION

View Article Online
View Journal | View Issue

Cite this: *Dalton Trans.*, 2020, **49**, 8836

Received 13th March 2020,
Accepted 2nd June 2020

DOI: 10.1039/d0dt00943a

rsc.li/dalton

Building a robust 3D Ca-MOF by a new square Ca_4O SBU for purification of natural gas†

Falu Hu,[a,b] Zhengyi Di,[c] Mingyan Wu*[c] and Jing Li *[a,b]

For the first time, a new square Ca_4O SBU is introduced into a 3D Ca-MOF, $([MeNH_2]_2[Ca_4O(MTB)_2(EtOH)_4])\cdot(solvent)_n$ (1), to generate a (4,8)-connected flu-topology structure. Compound 1 exhibits selective adsorption of C_3 and C_2 hydrocarbons and CO_2 over CH_4 with especially high IAST selectivities for C_3 hydrocarbons over CH_4 (at 15/85 and 50/50 ratio) at 298K and 1 bar.

Metal–organic frameworks (MOFs) have become one of the most rapidly developing material classes over the past two decades, for their structural diversity and considerable potential for various applications, such as catalysis, drug delivery, gas storage and separation, and luminescence based chemical sensing.[1–15] MOFs are built from metal ions or SBUs as nodes and organic ligand as linkers, such as phosphonates, carboxylates, and sulfonates.[16] Among them, aromatic carboxylate anions are of particular interest because of their strong coordination ability toward many metal ions. Compared to the transition and lanthanide metal ion-based MOFs, structures constructed from alkaline earth metals such as Ca, especially those of 3D Ca-MOFs with permanent porosity, are much less explored.[17–29] This may be attributed to the inherent difficulties such as the unpredictable coordination geometries and high coordination number of Ca^{2+} ions. However, the calcium ions possess unique advantages, for example, being environment friendly, low-cost and large abundance in nature.[19,30] Therefore, designing new Ca-MOFs is beneficial to expand the scope of their applications.

On the other hand, natural gas is an important energy source with wide applications in industry. Thus, it is of significant importance to purify natural gas by the removal of CO_2 and higher C_2 and C_3 hydrocarbons from light CH_4. Porous materials (MOFs and HOFs) exhibit huge advantages for this separation process due to their well-defined structures, tunable pore sizes and open metal sites. Recently, we have done some work in the purification of natural gas using porous materials,[31–33] and we now expand this study to include Ca-MOFs and to assess their performance on the purification of natural gas.

According to hard and soft acid–base theory, since Ca^{2+} is a hard acid, we have selected a hard-base ligand in this work to facilitate the crystal growth of Ca-MOFs. 4,4′,4″,4‴-Methanetetrayltetrabenzoic acid (H_4MTB), a tetracarboxylic acid with a tetrahedral geometry has been previously used to synthesize a number of 3D MOFs,[34–38] but no work has been reported on Ca-based structures using this ligand. In this study, we succeeded in obtaining a 3D Ca-MTB MOF, $[Me_2NH_2]_2[Ca_4O(MTB)_2(CH_3CH_2OH)_4]\cdot(solvent)_n$ (**1**). Compound **1** represents the first example where the framework is built on a square Ca_4O SBU with a (4,8)-connected **flu**-topology. We analysed its porosity and investigated its gas adsorption properties and potential for natural gas purification.

$[Me_2NH_2]_2[Ca_4O(MTB)_2(CH_3CH_2OH)_4]\cdot(solvent)_n$ (**1**) was synthesized *via* solvothermal reactions of $Ca(NO_3)_2\cdot4H_2O$ and H_4MTB in the mixture solvents of DMF and EtOH at 80 °C for 5 days. The single crystal X-ray diffraction analysis indicates that **1** crystallizes in the tetragonal system, space group *I*4/*m*. In the asymmetric unit of **1**, there is one-half Ca^{2+} ion, one-fourth MTB^{4-}, one-eighth O^{2-} and one-half coordinated EtOH. Thus, the framework is negatively charged. Each Ca^{2+} is surrounded by eight O atoms including six O atoms from carboxylic groups and one O atom from EtOH and one O atom from μ_4-O^{2-}, which yields a coordination geometry of a trigonal dodecahedron (Fig. S1†). The H_4MTB ligand is completely deprotonated and forms MTB^{4-}. The μ_4-O^{2-} links four Ca^{2+} ions to generate a Ca_4O SBU with a square planar geometry (Fig. S2a†), which is very different from most previously

[a]*Hoffmann Institute of Advanced Materials, Shenzhen Polytechnic, 7098 Liuxian Blvd, Nanshan District, Shenzhen, 518055, China*
[b]*Department of Chemistry and Chemical Biology, Rutgers University, 123 Bevier Road, Piscataway, NJ, 08854, USA. E-mail: jingli@rutgers.edu*
[c]*State Key Laboratory of Structure Chemistry, Fujian Institute of Research on the Structure of Matter, Chinese Academy of Sciences, Fuzhou, 350002, China. E-mail: wumy@fjirsm.ac.cn*

†Electronic supplementary information (ESI) available. CCDC 1983688. For ESI and crystallographic data in CIF or other electronic format see DOI: 10.1039/D0DT00943A

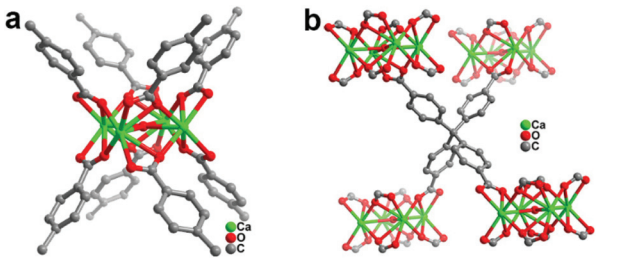

Fig. 1 (a) The 8-connected Ca_4O SBU. (b) The coordination of the tetrahedral ligand. H atoms and terminal solvent are omitted for clarity.

reported metal coordination modes.[39–47] Although similar M_4O (M = Cu, Zn, Co, Mn, Cd, Be, and Mg) SBUs have been reported,[48–56] to the best of our knowledge, it is the first time to introduce the square Ca_4O SBU into the (4,8)-connected 3D Ca-MOF.

As shown in Fig. 1b, each tetrahedral ligand is surrounded by four Ca_4O SBUs and links to eight Ca^{2+} ions by using μ_2-O1:μ_1-O2 coordinated mode from four deprotonated carboxylic groups. Each planar Ca_4O SBU (secondary building unit) is connected by eight carboxylate groups above and below the plane *via* coordination modes μ_2-O1:μ_1-O2 from eight MTB^{4-} ligands (Fig. 1a), similar to the reported structure of $[Cd_4(O_2CR)_8]$.[57] The eight MTB^{4-} ligands and six Ca_4O SBUs form an octahedron cage (Fig. 2a). The pore diameter of the cage is about 19.5 × 24.9 Å, when estimated through the distance of two opposite vertexes. The octahedron cages are further packed into a 3D framework (Fig. 2b). There are two different channels along the (1 1 1) direction of the framework: 6.0 Å × 3.6 Å (O2–O2 and H7–H7, respectively) and 6.5 Å × 5.6 Å (O1–O1 and H8–H8, respectively) taking into account the VDW radii (H: 1.2 Å; C: 1.7 Å; O: 1.5 Å). In addition, parallel to the *a* or *b* axis also exists two different pores 3.2 Å x 6.2 Å (H4–H4 and C5–C2, respectively) with VDW radii taken into consideration. The pore between two opposite vertexes is about 12.4 × 8.2 Å, with two coordinated EtOH molecules included in the pore space. Considering MTB^{4-} ligand as a tetrahedral four-connected node and Ca_4O SBU simplified as the eight-connected node, the topological analysis of **1** reveals that the structure is a **flu** topology with the point symbol of $\{4^12.6^12.8^4\}\{4^6\}_2$ using TOPOS 4.0 program package (Fig. 2c).[58] The solvent accessible volume in fully evacuated **1** is about 42.9% (without considering the counter ions), estimated by PLATON.[59] The PXRD pattern of the bulk sample **1** matches well with the simulated one, indicating the sample has high purity (Fig. S3†). TGA analyses of the as-made and activated samples show that both are stable up to 480 °C, indicating the high thermal stability of the framework (Fig. S6†).

N_2 adsorption was carried out on a 3-Flex system to analyse the porosity of **1**. Before the gas adsorption experiment, the activated sample was prepared by soaking the crystals of **1** in EtOH for 3 days. N_2 adsorption isotherm obtained at 77 K exhibits a typical type-I adsorption behaviour, indicating the micropore nature of this MOF. The BET surface area was estimated to be 531.8 $m^2\ g^{-1}$ (Fig. S7†). The pore volume is 0.24 $cm^3\ g^{-1}$. The pore size distribution analysis indicates that there are three types of pores in the range of 5.6–6.1 Å (Fig. S8†). The results are almost consistent with the estimated pore dimensions based on the single crystal structure. Taking into consideration the pore sizes, adsorption experiments were then performed on a number of small gases including CO_2, C_2H_6, C_2H_4, C_2H_2, C_3H_8, C_3H_6, and C_3H_4 at 298 K and 1 bar. The adsorbed amounts of CO_2, C_2H_6, C_2H_4, C_2H_2, C_3H_8, C_3H_6 and C_3H_4 are 47.6, 44.9, 41.9, 53.5, 36.7, 47.9 and 58.1 $cm^3\ g^{-1}$, respectively, while the adsorption of CH_4 is only 11.9 $cm^3\ g^{-1}$ (Fig. 3a–c).

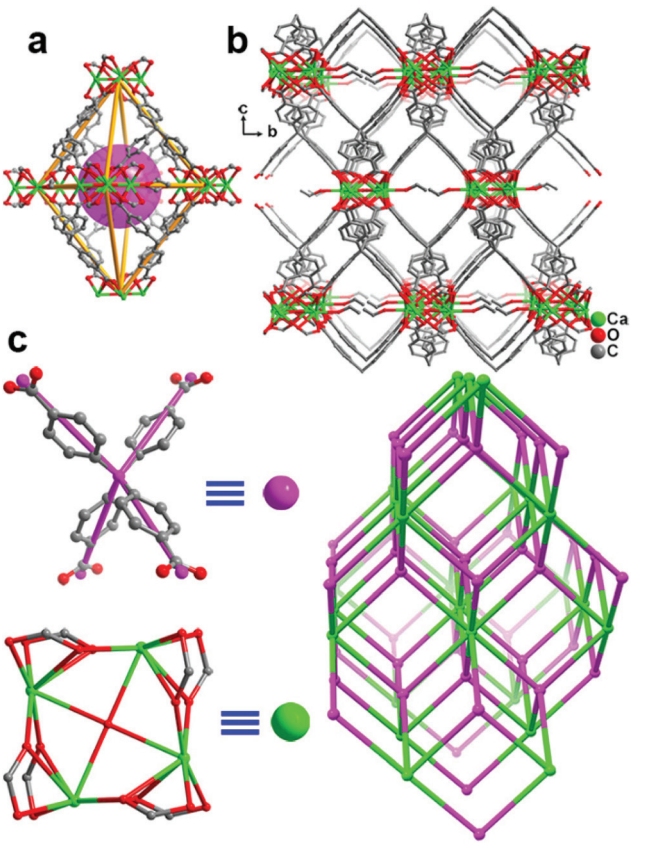

Fig. 2 (a) The octahedron cage. (b) The 3D porous structure. (c) The 4-connected node of ligand and 8-connected node of Ca_4O SBU and topological structure. (H atoms and terminal solvent are omitted for clarity).

The different adsorption capacities and the slopes of CO_2, C_2, or C_3 over CH_4 encouraged us to explore the selectivity of the various gases over CH_4. Single-component gas adsorption isotherms were used to calculate the selectivity based on the ideal adsorbed solution theory (IAST). At 298 K and 1 bar, the calculated CO_2/CH_4, C_3H_8/CH_4, C_3H_6/CH_4, C_3H_4/CH_4, C_2H_6/CH_4, C_2H_4/CH_4, and C_2H_2/CH_4 (at 15 : 85/50 : 50) adsorption selectivities of **1** are 6.3/6.8, 502.3/261.4, 140.1/91.3, 422.4/302, 21.4/17.3, 12.4/13.8 and 14.2/10.9, respectively (Fig. 4a–c and Fig. S9†). The results indicate that the selectivities of C_3 hydrocarbons over CH_4 are much higher than those of C_2 hydro-

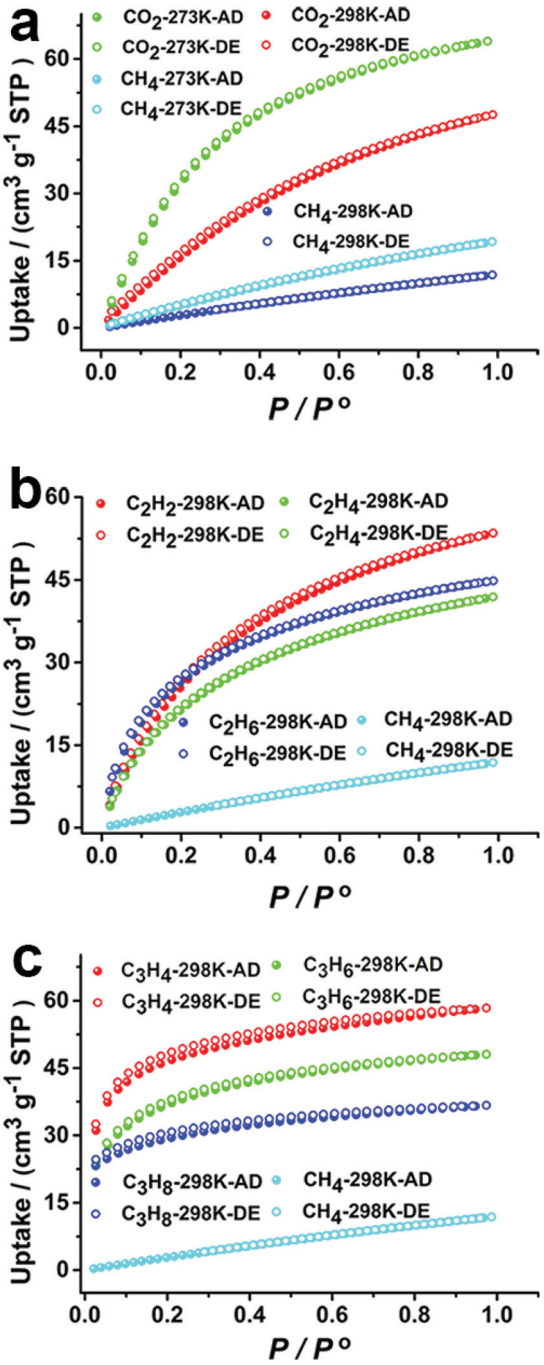

Fig. 3 (a)–(c) The sorption isotherms of **1** for CO_2, CH_4, C_2 and C_3 hydrocarbons.

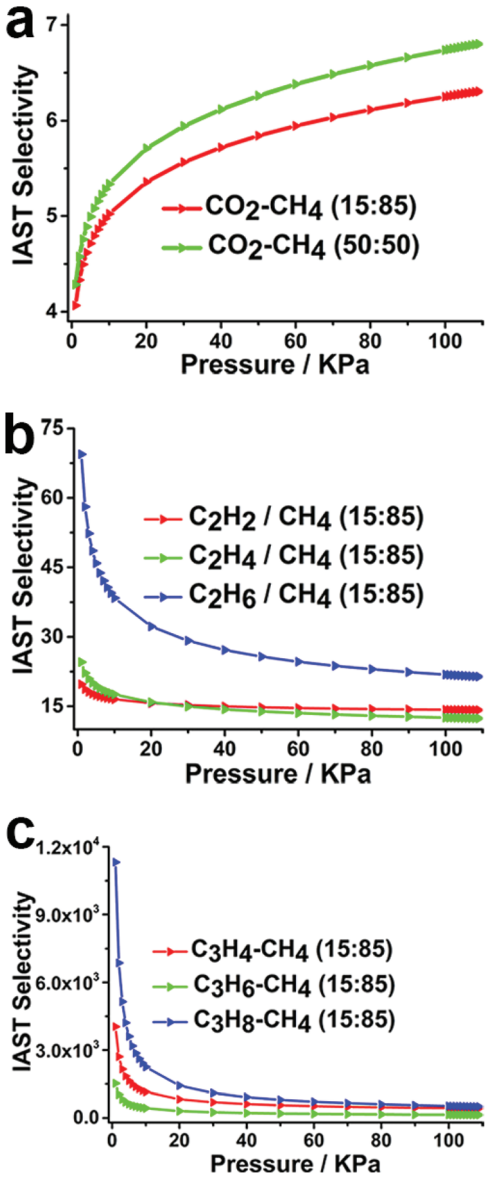

Fig. 4 (a)–(c) IAST predicted (15 : 85 or 50 : 50) gas mixture adsorption selectivity for **1** at 298 K and 1 bar.

carbons over CH_4 and CO_2 over CH_4. Although the adsorption capacities of C_3 hydrocarbons are lower than those of reported, the selectivities are among the highest values of MOFs, such as FJI-C4 (C_3H_8/CH_4: 294),[60] BSF-1 (C_3H_8/CH_4: 353),[61] JLU-Liu6 (C_3H_8/CH_4: 274.6),[62] JLU-Liu22 (C_3H_8/CH_4: 271.5),[63] UPC-100-In (C_3H_8/CH_4: 186.4; C_3H_6/CH_4: 200.5),[64] and UPC-104 (C_3H_6/CH_4: 97.9) (Tables S3 and S5†).[65]

The selectivities of C_2 over CH_4 are lower than that of FJI-C4 and ZJU-31a, but are higher than those of UTSA-33a,[66] UPC-33,[67] UPC-32,[68] ZJNU-61a,[69] MFM-202a,[70] UiO-67,[71] FIR-7a-ht,[72] FJI-C1,[73] and UTSA-36a (Table S5†).[74] The selectivities of CO_2/CH_4 are higher than those of SIFSIX-2-Cu (5.3),[75] ZIF-100 (5.9),[76] JLU-Liu5 (4.6),[62] JLU-Liu18 (5.4/4.5)[77] and Yb-BPT (3.1),[78] and comparable with those of UPC-33 (8.09),[67] UPC-32 (6.6),[68] USTA-61a (7.4),[79] PCN-88 (7.0)[80] and BSF-1 (7.5) (Table S5†).[61] We also estimated the isosteric heats of adsorption (Q_{st}) as a function of gas uptake amounts (Fig. S10†). The values obtained near zero coverage are the following: CO_2: 21.7 kJ mol^{-1}, C_2H_2: 24.5 kJ mol^{-1}, C_2H_4: 24.3 kJ mol^{-1}, C_2H_6: 23.3 kJ mol^{-1}, and C_3H_4: 90.9 kJ mol^{-1}. All of them are higher than that of CH_4, 15.2 kJ mol^{-1}. These results confirm that the extent of interactions of C2–C3 hydrocarbons and CO_2 with the host framework are stronger than that of CH_4. Furthermore,

breakthrough experiments were carried out for the binary mixtures of CO_2/CH_4, C_2H_6/CH_4 and C_3H_8/CH_4 (15 : 85). Good separation performance was achieved in all three cases (Fig. S11†).

In summary, we have synthesized and structurally characterized an unprecedented square Ca_4O SBU-based 3D Ca-MOF using a tetrahedral ligand. Compound **1** is a (4,8)-connected **flu** topological structure. The 3D Ca-MOF exhibits good selectivity of CO_2, C_2 and C_3 hydrocarbons over CH_4. Further studies to design and functionalize 3D Ca-MOFs for improved performance in efficient purification of natural gas is on the way.

Conflicts of interest

There are no conflicts to declare.

Acknowledgements

F. L. Hu acknowledges the support from the Hoffmann Institute of Advanced Materials (HIAM), Shenzhen Polytechnic, China.

Notes and references

1 J. Lee, O. K. Farha, J. Roberts, K. A. Scheidt, S. T. Nguyen and J. T. Hupp, *Chem. Soc. Rev.*, 2009, **38**, 1450–1459.
2 W. Zhu, J. Guo, Y. Ju, R. E. Serda, J. G. Croissant, J. Shang, E. Coker, J. O. Agola, Q. Z. Zhong, Y. Ping, F. Caruso and C. J. Brinker, *Adv. Mater.*, 2019, **31**, 1806774.
3 J. R. Li, R. J. Kuppler and H. C. Zhou, *Chem. Soc. Rev.*, 2009, **38**, 1477–1504.
4 K. Tan, S. Jensen, S. Zuluaga, E. K. Chapman, H. Wang, R. Rahman, J. Cure, T. H. Kim, J. Li, T. Thonhauser and Y. J. Chabal, *J. Am. Chem. Soc.*, 2018, **140**, 856–859.
5 W. G. Cui, T. L. Hu and X. H. Bu, *Adv. Mater.*, 2020, **32**, 1806445.
6 R.-B. Lin, S. Xiang, H. Xing, W. Zhou and B. Chen, *Coord. Chem. Rev.*, 2019, **378**, 87–103.
7 A. M. Plonka, X. Chen, H. Wang, R. Krishna, X. Dong, D. Banerjee, W. R. Woerner, Y. Han, J. Li and J. B. Parise, *Chem. Mater.*, 2016, **28**, 1636–1646.
8 B. R. Barnett, M. I. Gonzalez and J. R. Long, *Trends Chem.*, 2019, **1**, 159–171.
9 H. Li, K. Wang, Y. Sun, C. T. Lollar, J. Li and H.-C. Zhou, *Mater. Today*, 2018, **21**, 108–121.
10 H. Wang and J. Li, *Acc. Chem. Res.*, 2019, **52**, 1968–1978.
11 X. Zhao, Y. Wang, D. S. Li, X. Bu and P. Feng, *Adv. Mater.*, 2018, **30**, 1705189.
12 H. Wang, W. P. Lustig and J. Li, *Chem. Soc. Rev.*, 2018, **47**, 4729–4756.
13 W. P. Lustig, S. Mukherjee, N. D. Rudd, A. V. Desai, J. Li and S. K. Ghosh, *Chem. Soc. Rev.*, 2017, **46**, 3242–3285.
14 Z. Hu, B. J. Deibert and J. Li, *Chem. Soc. Rev.*, 2014, **43**, 5815–5840.
15 H. Wu, Q. Gong, D. H. Olson and J. Li, *Chem. Rev.*, 2012, **112**, 836–868.
16 W.-X. Zhang, P.-Q. Liao, R.-B. Lin, Y.-S. Wei, M.-H. Zeng and X.-M. Chen, *Coord. Chem. Rev.*, 2015, **293–294**, 263–278.
17 A. Mallick, E.-M. Schön, T. Panda, K. Sreenivas, D. D. Díaz and R. Banerjee, *J. Mater. Chem.*, 2012, **22**, 14951–14963.
18 C. Lv, W. Li, Y. Zhou, J. Li and Z. Lin, *Inorg. Chem. Commun.*, 2019, **99**, 40–43.
19 D. Banerjee, Z. Zhang, A. M. Plonka, J. Li and J. B. Parise, *Cryst. Growth Des.*, 2012, **12**, 2162–2165.
20 A. Douvali, G. S. Papaefstathiou, M. P. Gullo, A. Barbieri, A. C. Tsipis, C. D. Malliakas, M. G. Kanatzidis, I. Papadas, G. S. Armatas, A. G. Hatzidimitriou, T. Lazarides and M. J. Manos, *Inorg. Chem.*, 2015, **54**, 5813–5826.
21 S. Noro, J. Mizutani, Y. Hijikata, R. Matsuda, H. Sato, S. Kitagawa, K. Sugimoto, Y. Inubushi, K. Kubo and T. Nakamura, *Nat. Commun.*, 2015, **6**, 5851.
22 R. K. Alavijeh, K. Akhbari and J. White, *Cryst. Growth Des.*, 2019, **19**, 7290–7297.
23 M. Mazaj, G. Mali, M. Rangus, E. Žunkovič, V. Kaučič and N. Z. Logar, *J. Phys. Chem. C*, 2013, **117**, 7552–7564.
24 S.-C. Chen, F. Tian, K.-L. Huang, C.-P. Li, J. Zhong, M.-Y. He, Z.-H. Zhang, H.-N. Wang, M. Du and Q. Chen, *CrystEngComm*, 2014, **16**, 7673–7680.
25 S. R. Miller, E. Alvarez, L. Fradcourt, T. Devic, S. Wuttke, P. S. Wheatley, N. Steunou, C. Bonhomme, C. Gervais, D. Laurencin, R. E. Morris, A. Vimont, M. Daturi, P. Horcajada and C. Serre, *Chem. Commun.*, 2013, **49**, 7773–7775.
26 J. Yang, C. A. Trickett, S. B. Alahmadi, A. S. Alshammari and O. M. Yaghi, *J. Am. Chem. Soc.*, 2017, **139**, 8118–8121.
27 A. Mallick, T. Kundu and R. Banerjee, *Chem. Commun.*, 2012, **48**, 8829–8831.
28 F. J. Zhao, Y. X. Tan, W. Wang, Z. Ju and D. Yuan, *Inorg. Chem.*, 2018, **57**, 13312–13317.
29 D. Kojima, T. Sanada, N. Wada and K. Kojima, *RSC Adv.*, 2018, **8**, 31588–31593.
30 J.-C. Zhang, J.-J. Wang, S.-L. Zeng, Z.-M. Wang, Y. Liu, D.-J. Zhang, R.-C. Zhang and Y. Fan, *Inorg. Chem. Commun.*, 2018, **97**, 69–73.
31 F. Hu, C. Liu, M. Wu, J. Pang, F. Jiang, D. Yuan and M. Hong, *Angew. Chem., Int. Ed.*, 2017, **56**, 2101–2104.
32 F. Hu, P. Huang, Z. Di, M. Wu, F. Jiang and M. Hong, *Chem. Commun.*, 2019, **55**, 10257–10260.
33 F. Hu, Z. Di, M. Wu, M. Hong and J. Li, *Cryst. Growth Des.*, 2019, **19**, 6381–6387.
34 M. Almasi, V. Zelenak, A. Zukal, J. Kuchar and J. Cejka, *Dalton Trans.*, 2016, **45**, 1233–1242.
35 M. Almasi, V. Zelenak, M. Opanasenko and J. Cejka, *Dalton Trans.*, 2014, **43**, 3730–3738.
36 H. Furukawa, F. Gandara, Y. B. Zhang, J. Jiang, W. L. Queen, M. R. Hudson and O. M. Yaghi, *J. Am. Chem. Soc.*, 2014, **136**, 4369–4381.
37 G. Xing, T. Yan, S. Das, T. Ben and S. Qiu, *Angew. Chem., Int. Ed.*, 2018, **57**, 5345–5349.

38 I. Bassanetti, S. Bracco, A. Comotti, M. Negroni, C. Bezuidenhout, S. Canossa, P. P. Mazzeo, L. Marchió and P. Sozzani, *J. Mater. Chem. A*, 2018, **6**, 14231–14239.
39 S. A. Diamantis, A. D. Pournara, A. G. Hatzidimitriou, M. J. Manos, G. S. Papaefstathiou and T. Lazarides, *Polyhedron*, 2018, **153**, 173–180.
40 P.-C. Liang, H.-K. Liu, C.-T. Yeh, C.-H. Lin and V. t. z. Zima, *Cryst. Growth Des.*, 2011, **11**, 699–708.
41 A. Margariti, S. Rapti, A. D. Katsenis, T. Friščić, Y. Georgiou, M. J. Manos and G. S. Papaefstathiou, *Inorg. Chem. Front.*, 2017, **4**, 773–781.
42 M. K. Kim, K.-L. Bae and K. M. Ok, *Cryst. Growth Des.*, 2011, **11**, 930–932.
43 A. M. Plonka, D. Banerjee and J. B. Parise, *Cryst. Growth Des.*, 2012, **12**, 2460–2467.
44 R. K. Vakiti, B. D. Garabato, N. P. Schieber, M. J. Rucks, Y. Cao, C. Webb, J. B. Maddox, A. Celestian, W.-P. Pan and B. Yan, *Cryst. Growth Des.*, 2012, **12**, 3937–3943.
45 Z. W. Wei, C. X. Chen, S. P. Zheng, H. P. Wang, Y. N. Fan, Y. Y. Ai, M. Pan and C. Y. Su, *Inorg. Chem.*, 2016, **55**, 7311–7313.
46 X. Zhang, Y.-Y. Huang, M.-J. Zhang, J. Zhang and Y.-G. Yao, *Cryst. Growth Des.*, 2012, **12**, 3231–3238.
47 W. M. Liao, J. H. Zhang, S. Y. Yin, H. Lin, X. Zhang, J. Wang, H. P. Wang, K. Wu, Z. Wang, Y. N. Fan, M. Pan and C. Y. Su, *Nat. Commun.*, 2018, **9**, 2401.
48 L. M. Yang, G. Y. Fang, J. Ma, R. Pushpa and E. Ganz, *Phys. Chem. Chem. Phys.*, 2016, **18**, 32319–32330.
49 L. M. Yang, P. Ravindran and M. Tilset, *Inorg. Chem.*, 2013, **52**, 4217–4228.
50 C. Heering, I. Boldog, V. Vasylyeva, J. Sanchiz and C. Janiak, *CrystEngComm*, 2013, **15**, 9757–9768.
51 W. H. Fang, L. Zhang, J. Zhang and G. Y. Yang, *Chem. Commun.*, 2015, **51**, 17174–17177.
52 X. M. Zhang, J. Lv, F. Ji, H. S. Wu, H. Jiao and P. Schleyer, *J. Am. Chem. Soc.*, 2011, **133**, 4788–4790.
53 J. J. t. Perry, J. A. Perman and M. J. Zaworotko, *Chem. Soc. Rev.*, 2009, **38**, 1400–1417.
54 S. Hausdorf, F. Baitalow, T. Böhle, D. Rafaja and F. O. R. L. Mertens, *J. Am. Chem. Soc.*, 2010, **132**, 10978–10981.
55 H. Yang, M. Luo, Z. Wu, W. Wang, C. Xue and T. Wu, *Chem. Commun.*, 2018, **54**, 11272–11275.
56 J. An, O. K. Farha, J. T. Hupp, E. Pohl, J. I. Yeh and N. L. Rosi, *Nat. Commun.*, 2012, **3**, 604.
57 H. Chun, D. Kim, D. N. Dybtsev and K. Kim, *Angew. Chem., Int. Ed.*, 2004, **43**, 971–974.
58 V. A. Blatov, A. P. Shevchenko and D. M. Proserpio, *Cryst. Growth Des.*, 2014, **14**, 3576–3586.
59 A. L. Spek, *J. Appl. Crystallogr.*, 2003, **36**, 7–13.
60 L. Li, X. Wang, J. Liang, Y. Huang, H. Li, Z. Lin and R. Cao, *ACS Appl. Mater. Interfaces*, 2016, **8**, 9777–9781.
61 Y. Zhang, L. Yang, L. Wang, S. Duttwyler and H. Xing, *Angew. Chem., Int. Ed.*, 2019, **58**, 8145–8150.
62 D. Wang, T. Zhao, Y. Cao, S. Yao, G. Li, Q. Huo and Y. Liu, *Chem. Commun.*, 2014, **50**, 8648–8650.
63 D. Wang, B. Liu, S. Yao, T. Wang, G. Li, Q. Huo and Y. Liu, *Chem. Commun.*, 2015, **51**, 15287–15289.
64 W. Fan, X. Wang, B. Xu, Y. Wang, D. Liu, M. Zhang, Y. Shang, F. Dai, L. Zhang and D. Sun, *J. Mater. Chem. A*, 2018, **6**, 24486–24495.
65 W. Fan, X. Liu, X. Wang, Y. Li, C. Xing, Y. Wang, W. Guo, L. Zhang and D. Sun, *Inorg. Chem. Front.*, 2018, **5**, 2445–2449.
66 Y. He, Z. Zhang, S. Xiang, F. R. Fronczek, R. Krishna and B. Chen, *Chem. – Eur. J.*, 2012, **18**, 613–619.
67 W. Fan, Y. Wang, Q. Zhang, A. Kirchon, Z. Xiao, L. Zhang, F. Dai, R. Wang and D. Sun, *Chem. – Eur. J.*, 2018, **24**, 2137–2143.
68 W. Fan, Y. Wang, Z. Xiao, Z. Huang, F. Dai, R. Wang and D. Sun, *Chin. Chem. Lett.*, 2018, **29**, 865–868.
69 Y. Ling, J. Jiao, M. Zhang, H. Liu, D. Bai, Y. Feng and Y. He, *CrystEngComm*, 2016, **18**, 6254–6261.
70 S. Gao, C. G. Morris, Z. Lu, Y. Yan, H. G. W. Godfrey, C. Murray, C. C. Tang, K. M. Thomas, S. Yang and M. Schröder, *Chem. Mater.*, 2016, **28**, 2331–2340.
71 Y. Zhang, H. Xiao, X. Zhou, X. Wang and Z. Li, *Ind. Eng. Chem. Res.*, 2017, **56**, 8689–8696.
72 Y. P. He, Y. X. Tan and J. Zhang, *Chem. Commun.*, 2013, **49**, 11323–11325.
73 Y. Huang, Z. Lin, H. Fu, F. Wang, M. Shen, X. Wang and R. Cao, *ChemSusChem*, 2014, **7**, 2647–2653.
74 M. C. Das, H. Xu, S. Xiang, Z. Zhang, H. D. Arman, G. Qian and B. Chen, *Chem. – Eur. J.*, 2011, **17**, 7817–7822.
75 P. Nugent, Y. Belmabkhout, S. D. Burd, A. J. Cairns, R. Luebke, K. Forrest, T. Pham, S. Ma, B. Space, L. Wojtas, M. Eddaoudi and M. J. Zaworotko, *Nature*, 2013, **495**, 80–84.
76 B. Wang, A. P. Cote, H. Furukawa, M. O'Keeffe and O. M. Yaghi, *Nature*, 2008, **453**, 207–211.
77 S. Yao, D. Wang, Y. Cao, G. Li, Q. Huo and Y. Liu, *J. Mater. Chem. A*, 2015, **3**, 16627–16632.
78 Z. Guo, H. Xu, S. Su, J. Cai, S. Dang, S. Xiang, G. Qian, H. Zhang, M. O'Keeffe and B. Chen, *Chem. Commun.*, 2011, **47**, 5551–5553.
79 Y. He, H. Furukawa, C. Wu, M. O'Keeffe and B. Chen, *CrystEngComm*, 2013, **15**, 9328–9331.
80 J. R. Li, J. Yu, W. Lu, L. B. Sun, J. Sculley, P. B. Balbuena and H. C. Zhou, *Nat. Commun.*, 2013, **4**, 1538.